Published in final edited form as:
Neuropharmacology. 2014 April ; 79: 172–179. doi:10.1016/j.neuropharm.2013.10.018.

Synaptic gene dysregulation within hippocampal CA1 pyramidal neurons in mild cognitive impairment

Scott E. Counts[1,5], **Melissa J. Alldred**[2,3], **Shaoli Che**[2,3], **Stephen D. Ginsberg**[2,3,4], and **Elliott J. Mufson**[1]

[1]Department of Neurological Sciences, Rush University Medical Center, Chicago, Illinois, USA

[2]Center for Dementia Research, Nathan Kline Institute, New York University School of Medicine, Orangeburg, New York, USA

[3]Department of Psychiatry, New York University School of Medicine, Orangeburg, New York, USA

[4]Department of Physiology and Neuroscience, New York University School of Medicine, Orangeburg, New York, USA

Abstract

Clinical neuropathologic studies suggest that the selective vulnerability of hippocampal CA1 pyramidal projection neurons plays a key role in the onset of cognitive impairment during the early phases of Alzheimer's disease (AD). Disruption of this neuronal population likely affects hippocampal pre- and postsynaptic efficacy underlying episodic memory circuits. Therefore, identifying perturbations in the expression of synaptic gene products within CA1 neurons prior to frank AD is crucial for the development of disease modifying therapies. Here we used custom-designed microarrays to examine progressive alterations in synaptic gene expression within CA1 neurons in cases harvested from the Rush Religious Orders Study who died with a clinical diagnosis of no cognitive impairment (NCI), mild cognitive impairment (MCI, a putative prodromal AD stage), or mild/moderate AD. Quantitative analysis revealed that 21 out of 28 different transcripts encoding regulators of synaptic function were significantly downregulated (1.4 to 1.8 fold) in CA1 neurons in MCI and AD compared to NCI, whereas synaptic transcript levels were not significantly different between MCI and AD. The downregulated transcripts encoded regulators of presynaptic vesicle trafficking, including synaptophysin and synaptogyrin, regulators of vesicle docking and fusion/release, such as synaptotagmin and syntaxin 1, and regulators of glutamatergic postsynaptic function, including PSD-95 and synaptopodin. Clinical pathologic correlation analysis revealed that downregulation of these synaptic markers was strongly associated with poorer antemortem cognitive status and postmortem AD pathological criteria such as Braak stage, NIA-Reagan, and CERAD diagnosis. In contrast to the widespread loss of synaptic gene expression observed in CA1 neurons in MCI, transcripts encoding β-amyloid precursor protein (APP), APP family members, and regulators of APP metabolism were not differentially regulated in CA1 neurons across the clinical diagnostic groups. Taken together,

Address correspondence to: Scott E. Counts, PhD or Elliott J. Mufson, PhD, Rush University Medical Center, 1735 West Harrison Street Suite 300, Chicago IL 60612, Phone 312-563-3570, Fax 312-563-3571, scott_e_counts@rush.edu; emufson@rush.edu.
[5]Current Address: Department of Translational Science and Molecular Medicine, Department of Family Medicine, Michigan State University, Grand Rapids, MI, USA

these data suggest that CA1 synaptic gene dysregulation occurs early in the cascade of pathogenic molecular events prior to the onset of AD, which may form the basis for novel pharmacological treatment approaches for this dementing disorder.

Keywords

Alzheimer's disease; gene regulation; hippocampus; microarray; mild cognitive impairment; synaptic

Introduction

Hippocampal neurodegeneration and synapse loss are prominent features of Alzheimer's disease (AD)(Hanks and Flood, 1991; Hyman et al., 1984; Scheff et al., 2005; West, 1993). In vivo imaging and clinical neuropathologic studies show that the hippocampal formation is one of the first sites to degenerate in mild cognitive impairment (MCI), a putative prodromal AD stage (deToledo-Morrell et al., 2007; Devanand et al., 2007; Scheff et al., 2007), suggesting that hippocampal disconnection is an early event underlying the clinical presentation of the disease. In this regard, CA1 pyramidal neurons comprise a differentially vulnerable hippocampal cell group, which may provide unique insight into defining mechanisms of synaptic failure early in AD, which remain unknown. Synaptic efficacy depends upon the intricate coordination of synaptic vesicle trafficking (e.g., targeting and docking, membrane fusion/exocytosis and endocytosis) and pre- and postsynaptic structure and plasticity (Kennedy et al., 2005; Murthy and De Camilli, 2003). Therefore, perturbations in the expression of synaptic gene products regulating these processes may play a role in the synaptic basis for hippocampal dysfunction during the progression of AD. Recent studies employing regional microarray analysis of hippocampal tissue (Berchtold et al., 2013) or single cell microarray analysis of CA1 neurons (Ginsberg et al., 2012; Ginsberg et al., 2000) revealed downregulation of multiple synaptic genes in aging and AD. However, whether alterations in CA1 synaptic gene expression differentiate aged, cognitively intact people from those with a preclinical diagnosis of MCI remains unclear. To address this question, we used custom microarrays to determine whether individual CA1 pyramidal neurons exhibit synaptic perturbations during the onset of cognitive decline. The CA1 neurons were accessed from postmortem hippocampus of subjects classified antemortem with no cognitive impairment (NCI), MCI or AD. These findings were correlated with performance on antemortem cognitive tests and postmortem neuropathologic criteria.

Materials and Methods

Subjects

This study was performed under IRB guidelines administrated by the Rush University Medical Center. Custom-designed microarray analysis of CA1 pyramidal neurons was performed using hippocampal tissue harvested postmortem from 35 participants in the Rush Religious Orders Study (Bennett et al., 2002) who were clinically diagnosed within a year of death with NCI (n = 12), MCI (n=15) or mild/moderate AD (n = 8; see Table 1). Details of clinical evaluations and diagnostic criteria have been previously published (Counts et al., 2006; Ginsberg et al., 2010; Mufson et al., 1999). In addition to an annual clinical evaluation, subjects were administered the Mini Mental State Exam and a battery of 19 neuropsychological tests referable to multiple cognitive domains (e.g., episodic memory, perceptual speed) (Mufson et al., 1999). A Global Cognitive Score (GCS), consisting of a composite z-score calculated from this test battery, was determined for each participant (Bennett et al., 2002). The MCI population was defined as subjects who exhibited cognitive

impairment on neuropsychological testing but who did not meet the clinical criteria for AD recommended by the joint working group of the National Institute of Neurologic and Communicative Disorders and Stroke/AD and Related Disorders Association (NINCDS/ADRDA)(Bennett et al., 2002; McKhann et al., 1984). These criteria are compatible with those used by experts in the field to describe subjects who are not cognitively normal but do not meet established criteria for dementia (Petersen et al., 2001).

The tissue samples were harvested using standardized accrual methods and procedures as previously reported (Counts et al., 2006; Ginsberg et al., 2010; Mufson et al., 1999). At autopsy, tissue blocks containing the hippocampal formation from one hemisphere were immersion-fixed in 4% paraformaldehyde in 0.1 M phosphate buffer, pH 7.2 for 24–72 h at 4 °C, paraffin embedded, and cut on a rotary microtome at 6 μm thickness. Tissue slabs from the opposite hemisphere were snap-frozen in liquid nitrogen for biochemical analysis. A series of tissue sections was prepared for neuropathological evaluation including visualization and quantitation of amyloid plaques and neurofibrillary tangles (NFTs) using antibodies directed against amyloid-β peptide (Aβ; 4 G8, Covance), thioflavine-S, modified Bielschowsky silver stain, and tau (PHF1, Gift from Dr. Peter Davies) (Bennett et al., 2002; Mufson et al., 1999), respectively. Additional sections were stained for Lewy bodies using antibodies directed against ubiquitin and α-synuclein. Exclusion criteria included argyrophilic grain disease, frontotemporal dementia, Lewy body disease, mixed dementias, Parkinson's disease, and stroke. A board certified neuropathologist blinded to the clinical diagnosis performed the neuropathological evaluation. Neuropathological designations were based on NIA-Reagan, CERAD and Braak staging criteria (Braak and Braak, 1991; Hyman et al., 2012; Mirra et al., 1991). Amyloid burden and apolipoprotein E (ApoE) genotype were determined for each case as described previously (Bennett et al., 2002; Mufson et al., 1999).

Tissue accrual for microarray analysis

Acridine orange histofluorescence (Ginsberg et al., 1997) and bioanalysis (Bioanalyzer 2100, Agilent Biotechnologies, Santa Clara, CA) (Alldred et al., 2009) were performed on each case to ensure that high quality RNA was present in hippocampal tissue sections. RNase-free precautions were used throughout the experimental procedures, and solutions were made with 18.2 mega Ohm RNase-free water (Nanopure Diamond, Barnstead, Dubuque, IA). Deparaffinized tissue sections were blocked in a 0.1 M Tris (pH 7.6) solution containing 2% donor horse serum (DHS; Sigma, St. Louis, MO) and 0.01% Triton X-100 for 1 hour and then incubated with a primary mouse monoclonal antibody directed against neurofilament subunits L, M, and H (1:200 dilution, RMdO20)(Lee et al., 1987) in a 0.1 M Tris/2% DHS solution overnight at 4 °C in a humidified chamber. Sections were processed with the ABC kit (Vector Labs, Burlingame, CA) and developed with 0.05% diaminobenzidine (Sigma), 0.03% hydrogen peroxide, and 0.01 M imidazole in Tris buffer for 10 minutes (Ginsberg et al., 2010). Tissue sections were not cover-slipped or counterstained and maintained in RNase-free 0.1 M Tris buffer solution. Individual CA1 pyramidal neurons were accessed by laser capture microdissection (LCM, Arcturus PixCell IIe, Life Technologies, Grand Island, NY). Fifty cells were captured per reaction for population cell analysis (Alldred et al., 2009; Alldred et al., 2012; Ginsberg et al., 2010). A total of 3–8 microarrays containing 50 LCM-captured CA1 neurons each were performed per case (Alldred et al., 2012).

TC RNA amplification

RNA amplification from CA1 neurons was performed using terminal continuation (TC) RNA amplification methodology (Che and Ginsberg, 2004; Ginsberg, 2005). The TC RNA amplification protocol is available at http://cdr.rfmh.org/pages/ginsberglabpage.html.

Microaspirated CA1 neurons were homogenized in 500 μl of Trizol reagent (Life Technologies). RNAs were reverse transcribed in the presence of the poly d(T) primer (100 ng/μl) and TC primer (100 ng/μl) in 1× first strand buffer (Life Technologies), 2 μg of linear acrylamide (Applied Biosystems), 10 mM dNTPs, 100 μM DTT, 20 U of SuperRNase Inhibitor (Life Technologies), and 200 U of reverse transcriptase (Superscript III, Life Technologies). Single-stranded cDNAs were digested with RNase H and re-annealed with the primers in a thermal cycler: RNase H digestion step at 37 °C, 30 minutes; denaturation step 95 °C, 3 minutes; primer re-annealing step 60 °C, 5 minutes. This step generated cDNAs with double-stranded regions at the primer interface. Samples were then purified by column filtration (Montage PCR filters; Millipore, Billerica, MA). Hybridization probes were synthesized by *in vitro* transcription using ^{33}P incorporation in 40 mM Tris (pH 7.5), 6 mM $MgCl_2$, 10 mM NaCl, 2 mM spermidine, 10 mM DTT, 2.5 mM ATP, GTP and CTP, 100 μM of cold UTP, 20 U of SuperRNase Inhibitor, 2 KU of T7 RNA polymerase (Epicentre, Madison, WI), and 120 μCi of ^{33}P-UTP (Perkin-Elmer, Boston, MA) (Alldred et al. 2012; Counts et al., 2009; Ginsberg et al., 2010). The labeling reaction was performed at 37 °C for 4 h. Radiolabeled TC RNA probes were hybridized to custom-designed microarrays without further purification.

Custom-designed microarray platforms and data analysis

Array platforms consisted of 1 μg of linearized cDNAs purified from plasmid preparations adhered to high-density nitrocellulose (Hybond XL, GE Healthcare) using an arrayer robot (VersArray, Bio-Rad, Hercules, CA). Approximately 576 cDNAs were utilized on the current array platform. Arrays were prehybridized (2 h) and hybridized (12 h) in a solution consisting of 6× saline–sodium phosphate–ethylenediaminetetraacetic acid (SSPE), 5× Denhardt's solution, 50% formamide, 0.1% sodium dodecyl sulfate (SDS), and denatured salmon sperm DNA (200 μg/ml) at 42 °C in a rotisserie oven (Che and Ginsberg, 2004; Counts et al., 2007; Ginsberg et al., 2010; Mufson et al., 2002). Following the hybridization protocol, arrays were washed sequentially in 2× SSC/0.1% SDS, 1× SSC/0.1% SDS and 0.5× SSC/0.1% SDS for 15 min each at 37 °C. Arrays were placed in a phosphor screen for 24 h and developed on a phosphor imager (GE Healthcare).

Data collection and statistical analysis for custom-designed microarrays

Hybridization signal intensity was determined utilizing ImageQuant software (GE Healthcare). Briefly, each array was compared to negative control arrays utilizing the respective protocols without any starting RNA. Expression of TC amplified RNA bound to each target minus background was then expressed as a ratio of the total hybridization signal intensity of the array (a global normalization approach). Global normalization effectively minimizes variation due to differences in the specific activity of the synthesized probe and the absolute quantity of probe (Eberwine et al., 2001; Ginsberg, 2008). We have previously demonstrated a linear relationship between TC-amplified RNA input concentration and mean hybridization signal intensity for individual and pooled cDNAs on a custom-designed array; hence, TC RNA amplification is a linear, reproducible process that preserves the original quantitative relationships of the mRNAs in individual neurons (Che and Ginsberg, 2004; Counts et al., 2007).

Relative changes in total hybridization signal intensity and in individual mRNAs were analyzed by one-way analysis of variance (ANOVA) with *post hoc* Newman-Keuls test for multiple comparisons. The level of statistical significance was set at $p < 0.01$ (Counts et al., 2009; Ginsberg, 2008; Ginsberg et al., 2010). False discovery rates were also estimated for the comparison of CA1 pyramidal neurons as described previously (Che and Ginsberg, 2004; Counts et al., 2007; Ginsberg, 2008). Expression levels were analyzed and clustered using bioinformatics and graphics software packages (GeneLinker Gold, Improved

Outcomes Inc., Kingston, ON and Accuprepress Inc., Torrance, CA). Expression levels of select transcripts were tested for associations with clinical pathological variables using Spearman rank correlations.

Quantitative PCR (qPCR)

qPCR was performed on frozen tissue micropunches containing either the hippocampal CA1 region or the cerebellum of 8 NCI, 6 MCI, and 8 AD cases from the Rush Religious Orders Study. Samples were assayed on a real-time PCR cycler (7900HT, Applied Biosystems) in 96-well optical plates as described previously (Alldred et al., 2009; Counts et al., 2007; Ginsberg, 2008). The ddCT method was employed to determine relative SYP, APP, SYN1, and SYT1 gene level differences with glyceraldehyde 3-phosphate dehydrogenase (GAPDH) qPCR products used as a control (Alldred et al., 2009; Counts et al., 2007; Ginsberg, 2008). Variance component analyses revealed relatively low levels of within-case variability, and the average value of the triplicate qPCR products from each case was used in subsequent analyses. Alterations in PCR product synthesis were analyzed by Kruskal-Wallis test with Bonferroni correction for post-hoc comparison. The level of statistical significance was set at 0.05 (two-sided).

Results

Subject demographics

Clinical and neuropathological characteristics of the 35 cases (12 NCI, 15 MCI, 8 mild/moderate AD) included in the microarray analysis are summarized in Table I. P-values were reported for descriptive purposes. No significant differences were observed for age, gender, educational level, or postmortem interval across the 3 groups. The ApoE ε4 allele was more frequent in AD compared to NCI and MCI cases. The mild/moderate AD group performed significantly poorer ($p < 0.0001$) on the MMSE compared to the NCI and MCI groups, whereas GCS *z*-scores were significantly progressively worse ($p < 0.0001$) during the transition from NCI to MCI to AD (see Table 1). Distribution of Braak scores was significantly different across clinical conditions, with NCI cases having lower Braak staging than MCI and AD. NCI cases were classified as Braak stages I–II (50%) and III–IV (50%). None of the NCI cases were stage V-VI. The MCI cohort displayed Braak stages I–II (6.6%), III–IV (66.7%), and V–VI (26.7%). By contrast, the AD cases were classified as Braak stages I–II (12.5%), III–IV (12.5%), and V–VI (75%), respectively (Table I). NIA-Reagan and CERAD criteria significantly differentiated NCI subjects from MCI and AD cases.

CA1 synaptic gene expression

Expression profiling was performed on a total of 161 custom-designed microarrays following the TC RNA amplification protocol. Quantitative analysis revealed differential regulation of 21 of 28 different transcripts encoding modulators of synaptic function. Notably, these 21 synaptic genes were all significantly downregulated in CA1 neurons in MCI compared to NCI, whereas synaptic transcript levels were not significantly different between MCI and AD (Fig. 1). The downregulated transcripts encoded several regulators of presynaptic vesicle trafficking, including synaptophysin (SYP; −1.8 fold change, NCI vs. MCI, AD; $p < 0.0001$), synaptobrevin (VAMP1; −1.7 fold; $p < 0.001$), and synaptogyrin (SYNGR1; −1.4 fold; $p < 0.0001$), as well as regulators of vesicle docking and fusion/release, such as synaptotagmin (SYT1; −1.5 fold; $p < 0.0001$) and several members of the syntaxin family (STX1, STX4, STX7; each −1.5 fold; $p < 0.0001$) (Fig. 1A). Gene products subserving glutamatergic postsynaptic function were significantly downregulated, including postsynaptic density protein 95 (PSD95, or DLG4; −1.5 fold; $p < 0.0001$), synaptopodin (SYNPO; −1.8 fold; $p < 0.0001$) and HOMER1 (−1.45 fold; $p < 0.001$) (Fig. 1B).

Regulators of synaptic clathrin-mediated endocytosis were also significantly downregulated in CA1 neurons in MCI and AD, including synaptojanin (SYNJ1; −1.6 fold; $p < 0.0001$) and adaptor-related protein complex 1 subunits (e.g., AP1G1; −1.35 fold; $p < 0.01$) (Fig. 1B). In contrast to the widespread loss of synaptic gene expression observed in CA1 neurons in MCI, transcripts encoding other functional classes of genes relevant to AD were unaffected. For instance, levels of amyloid-β precursor protein (APP) and several genes related to APP metabolism, such as beta-site APP-cleaving enzyme 1 (BACE1) and presenilin 1 (PSEN1), or APP family member genes (e.g., APLP1 and APLP2), were not differentially regulated in CA1 neurons across the clinical diagnostic groups (Fig. 1C).

Correlations with clinical pathologic variables

Select CA1 synaptic transcript levels were correlated with demographic data, antemortem cognitive test scores and postmortem neuropathologic variables. No associations were found between transcript levels and age or postmortem interval (data not shown). However, there was a very strong association between reductions in CA1 synaptic gene expression and poorer cognitive status as measured by each subject's GCS, the final composite z-score of the 19 neuropsychological tests administered prior to death (Fig. 2) (Bennett et al., 2002). In particular, the strongest associations were between GCS and presynaptic SYP ($p < 0.0001$) and SYT1 ($p < 0.0001$) and postsynaptic PSD95 ($p < 0.0001$) and SYNPO ($p < 0.0001$) transcripts. Pre- and postsynaptic transcripts also correlated with each other across the diagnostic groups (not shown), suggesting interrelated trans-synaptic disturbances during disease progression. Weaker but significant associations were also noted between synaptic gene expression levels and MMSE scores (Table 2). By comparison, stable levels of presynaptic modulators SYN1 and STX5 (Fig. 1) were not associated with GCS or MMSE scores (Fig. 2, Table 2) across the diagnostic groups. Virtually all of the select synaptic transcript reductions were negatively correlated with increasing measures of neuropathology as characterized by Braak, NIA-Reagan, and CERAD diagnostic criteria (Table 2). Notably, the postsynaptic markers PSD95 and SYNPO correlated more strongly with AD pathology than the presynaptic markers. In this regard, further analysis revealed that glutamatergic postsynaptic HOMER1 transcript levels were also strongly associated with GCS ($p < 0.0001$) as well as Braak ($p < 0.001$), NIA-Reagan ($p = 0.003$) and CERAD ($p = 0.01$) neuropathologic criteria (Table 2).

qPCR validation of microarray studies

Array data was validated by qPCR analysis of SYP and APP mRNA levels in frozen hippocampal CA1 enriched and cerebellar tissue from a subset of the cases. Similar to the single CA1 neuron expression profiling studies, SYP mRNA levels were significantly decreased ~40% in hippocampal samples from MCI and AD relative to NCI subjects ($p < 0.01$, Fig. 3A), whereas SYP levels in MCI and AD cases did not differ from each other. SYP mRNA levels in cerebellum were unchanged across the diagnostic groups (Fig. 3B). qPCR of APP transcripts also mirrored the custom microarray results, as levels were stable across the three groups in both hippocampus (Fig. 3C) and cerebellum (data not shown). Although CA1 SYN1 levels were stable across the groups via array data, qPCR analysis showed that SYN1 was down-regulated by ~30% in MCI and AD (Fig. 3D); this difference may reflect an admixture of regional hippocampal neurons or non-neuronal cell-types in the frozen micropunches. By contrast, qPCR confirmed the highly significant down-regulation of SYT1 as discovered by custom microarray analysis (Fig. 3E)

Discussion

Nearly 30 years have passed since it was hypothesized that neuronal disconnection in the hippocampal formation, a major component of the medial temporal memory circuit, is a

structural basis for dementia in AD (Hyman et al., 1984). Within the hippocampus, the CA1 pyramidal projection neurons develop neurofibrillary tangle pathology early in the disease onset (Braak and Braak, 1991). However, to date, the molecular alterations associated with CA1 pathology remains a mystery. Previously, we demonstrated that the expression of synaptic as well as other functional classes of genes is dysregulated in both unaffected and tangle-bearing hippocampal CA1 pyramidal neurons in mild/moderate and end-stage AD cases (Ginsberg et al., 2012; Ginsberg et al., 2000), supporting other microarray studies showing widespread alterations in multiple mRNA levels in frozen postmortem AD hippocampus (Blalock et al., 2011; Blalock et al., 2004; Colangelo et al., 2002). Here we show, for the first time, that the transition from normal cognition to MCI in aged individuals is marked by a specific and profound loss in the expression of gene products subserving synaptic function within this preferentially vulnerable CA cell group. Specifically, custom microarray analysis of RNA extracted from neurofilament-immunoreactive CA1 pyramidal neurons revealed an ~1.5-2-fold decrease in select transcripts encoding modulators of pre- and postsynaptic transmission in MCI subjects compared to NCI. Moreover, levels of these transcripts were not reduced any further in mild/moderate AD. By contrast, levels of APP-related gene products were stable in CA1 neurons in the clinical diagnostic groups examined. Taken together, these data suggest that synaptic dysregulation is a very early molecular pathogenic event which may play a role in the selective vulnerability of CA1 neurons and in the onset of cognitive decline seen during the prodromal phases of the disease process.

Among the synaptic genes dysregulated in CA1 neurons in MCI, reductions in transcripts mediating excitatory postsynaptic function, including PSD95, SYNPO and HOMER1, were most strongly associated with poorer antemortem cognitive performance and postmortem AD neuropathology. This finding tracks well with previous biochemical studies by our group and others showing that postsynaptic proteins such as PSD95 and drebrin are preferentially downregulated in the MCI hippocampus compared to cognitively normal subjects (Counts et al., 2012; Sultana et al., 2010). Moreover, our finding that SYNPO was the most severely dysregulated transcript in MCI and mild/moderate AD corresponds with a previous study showing that this molecule was the most down-regulated protein in the AD hippocampus compared to controls (Reddy et al., 2005). Similar to drebrin, SYNPO is an actin-associated protein that may play a role in modulating actin-based shape and motility of dendritic spines and seems to be essential for the formation of spine apparatuses involved in synaptic plasticity (Deller et al., 2003; Kremerskothen et al., 2005). Hence, the regulation of postsynaptic gene expression in vulnerable CA1 neurons may be critical to preserving hippocampal episodic memory function in the elderly.

Whether synaptic gene expression dysregulation underlies synaptic disconnection in the hippocampus or whether gene expression loss is concomitant with hippocampal synapse loss induced by other pathology (e.g., NFTs) remains an unanswered question. However, a comprehensive large-scale microarray analysis of multiple brain areas associated with cognition, including the hippocampus, revealed that there is a global and predominant down-regulation of synaptic-related genes in normal aging which is exacerbated AD (Berchtold et al.). Furthermore, human postmortem stereologic studies have shown that the dendritic extent of both apical and basal trees of CA1 neurons (Hanks and Flood, 1991), as well as CA1 neuron number (Freeman et al., 2008; West, 1993), is preserved in normal aging but that there is a dramatic loss in CA1 dendritic length (Hanks and Flood, 1991), synapse number (Scheff et al., 2005) and cell number (West, 1993) in AD. Hence, it appears that age-related dysregulation in hippocampal synaptic gene expression occurs in the absence of age-related morphological markers. On the other hand, several studies have shown that synaptic gene expression changes are concurrent with the development of NFTs in single CA1 neurons (Callahan and Coleman, 1995; Ginsberg et al., 2000), yet perturbations in

synaptic gene expression were also found even in CA1 neurons lacking thioflavin-S labeling in non-demented subjects with intermediate AD pathology (Braak stage II-IV) compared to those with little pathology (Braak stage 0-I) (Liang et al.). These data suggest instead that synaptic transcriptional dysregulation within CA1 neurons may precede frank NFT deposition and occur along with pre-tangle tau pathologic events. In this regard, we have found that synaptic genes are dysregulated in cholinergic basal forebrain (CBF) neurons labeled with the pS422 pretangle marker (Counts and Mufson, unpublished observations) and that pretangle formation within CBF neurons correlates with cognitive decline in MCI (Vana et al., 2011). Therefore, early tau pathological events may coincide with or foster early synaptic molecular pathology in AD, presaging CA1 morphological pathology during the progression of AD. A question remains as to where synaptic dysregulation occurs on the progression of dementia axis, and the present dataset indicates that MCI is truly a prodromal entity when considering downregulation of synaptic-related markers. Differential dysregulation of specific CA1 synaptic elements may even predict those MCI subjects who will most likely convert to frank AD. Additional quantitative morphometry and biochemical assessment of CA1 pyramidal neurons in MCI is warranted based upon the current findings.

In summary, molecular profiling of CA1 pyramidal neurons during the progression of AD reveals a prominent down-regulation of both pre-and postsynaptic transcripts in MCI which persists into the early stages of the disease. These incipient synaptic changes correlated strongly with antemortem cognitive decline, suggesting that they contribute to the selective vulnerability of this neuronal population and undermine the efficacy of glutamatergic transmission within the hippocampal episodic memory circuit. Given the involvement of tau in axonal transport, which is critical to synaptic function, the preferential formation of these lesions in the CA1 may be a salient pathogenic event driving synaptic gene dysregulation, CA1 cell loss, and synaptic loss in MCI. Therefore, these data may help form the basis for novel therapeutic approaches for the treatment of synaptic dysfunction during the prodromal stages of AD. To this end, therapeutic design must also consider evidence for the paradoxical up-regulation of synaptic elements with neocortical regions during MCI, which may reflect a plasticity response to mounting pathology and provide a rich source for understanding mechanisms of synaptic remodeling (Bell et al., 2007; Bossers et al., 2010; Counts et al., 2006; Williams et al., 2009). Future assessment of animal models of synaptic dissolution and/or models of differential regional synaptic pathology is desirable to identify mechanism(s) that underlie the selective transcriptional (as well as translational) dysregulation of synaptic-related markers.

Acknowledgments

We thank Irina Elarova, M.S., and Arthur Saltzman, M.S., for expert technical assistance. We are indebted to the altruism of the Rush Religious Orders Study participants. This study was supported by NIH grants PO1AG09466, P30AG10161, AG043375, AG42146, AG014449, AG17617, and the Alzheimer's Association (IIRG-12-237253).

Abbreviations

AD	Alzheimer's disease
AP1G1	adaptor-related protein complex 1, γ1 subunit
APBA1	APP-binding A1 protein
APBB1	APP-binding B1 protein
APLP1	APP-like protein 1
APLP2	APP-like protein 2

APP	amyloid-β precursor protein
APPBP1	APP-binding protein 1
BACE 1	beta-site APP-cleaving enzyme 1
CA1	Cornu Ammonis area 1
CERAD	Consortium to Establish a Registry for Alzheimer's Disease
CTNNB1	β-catenin
DLG3	Discs, Large Homolog 3 or synapse-associated protein, 102 kDa (SAP102)
DLG4	Discs, Large Homolog 4 or postsynaptic density protein, 95 kDa (PSD95)
ERBB2IP	Erb-B2, or Human Epidermal Growth Factor Receptor 2-interacting protein
GAP43	growth-associated protein, 43 kDa
GAPDH	glyceraldehyde 3-phosphate dehydrogenase
GCS	global cognitive score
HOMER1	Homer homolog 1
KCNIP3	Kv protein-interacting channel 3, or calsenilin
MCI	mild cognitive impairment
MMSE	Mini Mental State Exam
NCI	no cognitive impairment
PSEN1, 2	presenilin 1, 2
qPCR	quantitative polymerase chain reaction
SAP47	synapse-associated protein, 47 kDa;
SNAP29	synaptosomal-associated protein, 29 kDa
SNCA	α-synuclein
SNCB	β-synuclein
SNCAIP	α-synuclein-interacting protein
SNCG	γ-synuclein
STX1	4, 5, 7, syntaxin 1, 4, 5, 7
SYN1	synapsin 1
SYN3	synapsin 3
SYNGR	synaptogyrin
SYNJ	synaptojanin
SYNPO	synaptopodin
SYP	synaptophysin
SYT1	synaptotagmin 1
TC	terminal continuation
UTRN	utrophin
VAMP1	vesicle-associated membrane protein 1, or synaptobrevin 1

VPB	VAMP-associated protein B
VPP1	vesicle proton pump, 116 kDa

References

Alldred MJ, Che S, Ginsberg SD. Terminal continuation (TC) RNA amplification without second strand synthesis. J Neurosci Methods. 2009; 177:381–385. [PubMed: 19026688]

Alldred MJ, Duff KE, Ginsberg SD. Microarray analysis of CA1 pyramidal neurons in a mouse model of tauopathy reveals progressive synaptic dysfunction. Neurobiol Dis. 2012; 45:751–762. [PubMed: 22079237]

Bell KF, Bennett DA, Cuello AC. Paradoxical upregulation of glutamatergic presynaptic boutons during mild cognitive impairment. J Neurosci. 2007; 27:10810–10817. [PubMed: 17913914]

Bennett DA, Wilson RS, Schneider JA, Evans DA, Beckett LA, Aggarwal NT, Barnes LL, Fox JH, Bach J. Natural history of mild cognitive impairment in older persons. Neurology. 2002; 59:198–205. [PubMed: 12136057]

Berchtold NC, Coleman PD, Cribbs DH, Rogers J, Gillen DL, Cotman CW. Synaptic genes are extensively downregulated across multiple brain regions in normal human aging and Alzheimer's disease. Neurobiol Aging. 2013; 34:1653–1661. [PubMed: 23273601]

Blalock EM, Buechel HM, Popovic J, Geddes JW, Landfield PW. Microarray analyses of laser-captured hippocampus reveal distinct gray and white matter signatures associated with incipient Alzheimer's disease. J Chem Neuroanat. 2011; 42:118–126. [PubMed: 21756998]

Blalock EM, Geddes JW, Chen KC, Porter NM, Markesbery WR, Landfield PW. Incipient Alzheimer's disease: microarray correlation analyses reveal major transcriptional and tumor suppressor responses. Proc Natl Acad Sci U S A. 2004; 101:2173–2178. [PubMed: 14769913]

Bossers K, Wirz KT, Meerhoff GF, Essing AH, van Dongen JW, Houba P, Kruse CG, Verhaagen J, Swaab DF. Concerted changes in transcripts in the prefrontal cortex precede neuropathology in Alzheimer's disease. Brain. 2010; 133:3699–3723. [PubMed: 20889584]

Braak H, Braak E. Neuropathological stageing of Alzheimer-related changes. Acta Neuropathol. 1991; 82:239–259. [PubMed: 1759558]

Callahan LM, Coleman PD. Neurons bearing neurofibrillary tangles are responsible for selected synaptic deficits in Alzheimer's disease. Neurobiol Aging. 1995; 16:311–314. [PubMed: 7566340]

Che S, Ginsberg SD. Amplification of RNA transcripts using terminal continuation. Lab Invest. 2004; 84:131–137. [PubMed: 14647400]

Colangelo V, Schurr J, Ball MJ, Pelaez RP, Bazan NG, Lukiw WJ. Gene expression profiling of 12633 genes in Alzheimer hippocampal CA1: transcription and neurotrophic factor down-regulation and up-regulation of apoptotic and pro-inflammatory signaling. J Neurosci Res. 2002; 70:462–473. [PubMed: 12391607]

Counts SE, He B, Che S, Ginsberg SD, Mufson EJ. Galanin fiber hyperinnervation preserves neuroprotective gene expression in cholinergic basal forebrain neurons in Alzheimer's disease. J Alzheimers Dis. 2009; 18:885–896. [PubMed: 19749437]

Counts SE, He B, Che S, Ikonomovic MD, DeKosky ST, Ginsberg SD, Mufson EJ. Alpha7 nicotinic receptor up-regulation in cholinergic basal forebrain neurons in Alzheimer disease. Arch Neurol. 2007; 64:1771–1776. [PubMed: 18071042]

Counts SE, He B, Nadeem M, Wuu J, Scheff SW, Mufson EJ. Hippocampal drebrin loss in mild cognitive impairment. Neurodegener Dis. 2012; 10:216–219. [PubMed: 22310934]

Counts SE, Nadeem M, Lad SP, Wuu J, Mufson EJ. Differential expression of synaptic proteins in the frontal and temporal cortex of elderly subjects with mild cognitive impairment. J Neuropathol Exp Neurol. 2006; 65:592–601. [PubMed: 16783169]

Deller T, Korte M, Chabanis S, Drakew A, Schwegler H, Stefani GG, Zuniga A, Schwarz K, Bonhoeffer T, Zeller R, Frotscher M, Mundel P. Synaptopodin-deficient mice lack a spine apparatus and show deficits in synaptic plasticity. Proc Natl Acad Sci U S A. 2003; 100:10494–10499. [PubMed: 12928494]

deToledo-Morrell L, Stoub TR, Wang C. Hippocampal atrophy and disconnection in incipient and mild Alzheimer's disease. Prog Brain Res. 2007; 163:741–753. [PubMed: 17765748]

Devanand DP, Pradhaban G, Liu X, Khandji A, De Santi S, Segal S, Rusinek H, Pelton GH, Honig LS, Mayeux R, Stern Y, Tabert MH, de Leon MJ. Hippocampal and entorhinal atrophy in mild cognitive impairment: prediction of Alzheimer disease. Neurology. 2007; 68:828–836. [PubMed: 17353470]

Eberwine J, Kacharmina JE, Andrews C, Miyashiro K, McIntosh T, Becker K, Barrett T, Hinkle D, Dent G, Marciano P. mRna expression analysis of tissue sections and single cells. J Neurosci. 2001; 21:8310–8314. [PubMed: 11606616]

Freeman SH, Kandel R, Cruz L, Rozkalne A, Newell K, Frosch MP, Hedley-Whyte ET, Locascio JJ, Lipsitz LA, Hyman BT. Preservation of neuronal number despite age-related cortical brain atrophy in elderly subjects without Alzheimer disease. J Neuropathol Exp Neurol. 2008; 67:1205–1212. [PubMed: 19018241]

Ginsberg SD. RNA amplification strategies for small sample populations. Methods. 2005; 37:229–237. [PubMed: 16308152]

Ginsberg SD. Transcriptional profiling of small samples in the central nervous system. Methods Mol Biol. 2008; 439:147–158. [PubMed: 18370101]

Ginsberg SD, Alldred MJ, Che S. Gene expression levels assessed by CA1 pyramidal neuron and regional hippocampal dissections in Alzheimer's disease. Neurobiol Dis. 2012; 45:99–107. [PubMed: 21821124]

Ginsberg SD, Alldred MJ, Counts SE, Cataldo AM, Neve RL, Jiang Y, Wuu J, Chao MV, Mufson EJ, Nixon RA, Che S. Microarray analysis of hippocampal CA1 neurons implicates early endosomal dysfunction during Alzheimer's disease progression. Biol Psychiatry. 2010; 68:885–893. [PubMed: 20655510]

Ginsberg SD, Crino PB, Lee VM, Eberwine JH, Trojanowski JQ. Sequestration of RNA in Alzheimer's disease neurofibrillary tangles and senile plaques. Ann Neurol. 1997; 41:200–209. [PubMed: 9029069]

Ginsberg SD, Hemby SE, Lee VM, Eberwine JH, Trojanowski JQ. Expression profile of transcripts in Alzheimer's disease tangle-bearing CA1 neurons. Ann Neurol. 2000; 48:77–87. [PubMed: 10894219]

Hanks SD, Flood DG. Region-specific stability of dendritic extent in normal human aging and regression in Alzheimer's disease. I. CA1 of hippocampus. Brain Res. 1991; 540:63–82. [PubMed: 2054634]

Hyman BT, Phelps CH, Beach TG, Bigio EH, Cairns NJ, Carrillo MC, Dickson DW, Duyckaerts C, Frosch MP, Masliah E, Mirra SS, Nelson PT, Schneider JA, Thal DR, Thies B, Trojanowski JQ, Vinters HV, Montine TJ. National Institute on Aging-Alzheimer's Association guidelines for the neuropathologic assessment of Alzheimer's disease. Alzheimers Dement. 2012; 8:1–13. [PubMed: 22265587]

Hyman BT, Van Hoesen GW, Damasio AR, Barnes CL. Alzheimer's disease: cell-specific pathology isolates the hippocampal formation. Science. 1984; 225:1168–1170. [PubMed: 6474172]

Kennedy MB, Beale HC, Carlisle HJ, Washburn LR. Integration of biochemical signalling in spines. Nat Rev Neurosci. 2005; 6:423–434. [PubMed: 15928715]

Kremerskothen J, Plaas C, Kindler S, Frotscher M, Barnekow A. Synaptopodin, a molecule involved in the formation of the dendritic spine apparatus, is a dual actin/alpha-actinin binding protein. J Neurochem. 2005; 92:597–606. [PubMed: 15659229]

Lee VM, Carden MJ, Schlaepfer WW, Trojanowski JQ. Monoclonal antibodies distinguish several differentially phosphorylated states of the two largest rat neurofilament subunits (NF-H and NF-M) and demonstrate their existence in the normal nervous system of adult rats. J Neurosci. 1987; 7:3474–3488. [PubMed: 3119789]

Liang WS, Dunckley T, Beach TG, Grover A, Mastroeni D, Ramsey K, Caselli RJ, Kukull WA, McKeel D, Morris JC, Hulette CM, Schmechel D, Reiman EM, Rogers J, Stephan DA. Neuronal gene expression in non-demented individuals with intermediate Alzheimer's Disease neuropathology. Neurobiol Aging. 31:549–566. [PubMed: 18572275]

McKhann G, Drachman D, Folstein M, Katzman R, Price D, Stadlan EM. Clinical diagnosis of Alzheimer's disease: report of the NINCDS-ADRDA Work Group under the auspices of Department of Health and Human Services Task Force on Alzheimer's Disease. Neurology. 1984; 34:939–944. [PubMed: 6610841]

Mirra SS, Heyman A, McKeel D, Sumi SM, Crain BJ, Brownlee LM, Vogel FS, Hughes JP, van Belle G, Berg L. The Consortium to Establish a Registry for Alzheimer's Disease (CERAD). Part II. Standardization of the neuropathologic assessment of Alzheimer's disease. Neurology. 1991; 41:479–486. [PubMed: 2011243]

Mufson EJ, Chen EY, Cochran EJ, Beckett LA, Bennett DA, Kordower JH. Entorhinal cortex beta-amyloid load in individuals with mild cognitive impairment. Exp Neurol. 1999; 158:469–490. [PubMed: 10415154]

Mufson EJ, Counts SE, Ginsberg SD. Gene expression profiles of cholinergic nucleus basalis neurons in Alzheimer's disease. Neurochem Res. 2002; 27:1035–1048. [PubMed: 12462403]

Murthy VN, De Camilli P. Cell biology of the presynaptic terminal. Annu Rev Neurosci. 2003; 26:701–728. [PubMed: 14527272]

Petersen RC, Doody R, Kurz A, Mohs RC, Morris JC, Rabins PV, Ritchie K, Rossor M, Thal L, Winblad B. Current concepts in mild cognitive impairment. Arch Neurol. 2001; 58:1985–1992. [PubMed: 11735772]

Reddy PH, Mani G, Park BS, Jacques J, Murdoch G, Whetsell W Jr. Kaye J, Manczak M. Differential loss of synaptic proteins in Alzheimer's disease: implications for synaptic dysfunction. J Alzheimers Dis. 2005; 7:103–117. discussion 173-180. [PubMed: 15851848]

Scheff SW, Price DA, Schmitt FA, DeKosky ST, Mufson EJ. Synaptic alterations in CA1 in mild Alzheimer disease and mild cognitive impairment. Neurology. 2007; 68:1501–1508. [PubMed: 17470753]

Scheff SW, Price DA, Schmitt FA, Mufson EJ. Hippocampal synaptic loss in early Alzheimer's disease and mild cognitive impairment. Neurobiol Aging. 2005

Sultana R, Banks WA, Butterfield DA. Decreased levels of PSD95 and two associated proteins and increased levels of BCl2 and caspase 3 in hippocampus from subjects with amnestic mild cognitive impairment: Insights into their potential roles for loss of synapses and memory, accumulation of Abeta, and neurodegeneration in a prodromal stage of Alzheimer's disease. J Neurosci Res. 2010; 88:469–477. [PubMed: 19774677]

Vana L, Kanaan NM, Ugwu IC, Wuu J, Mufson EJ, Binder LI. Progression of tau pathology in cholinergic Basal forebrain neurons in mild cognitive impairment and Alzheimer's disease. Am J Pathol. 2011; 179:2533–2550. [PubMed: 21945902]

West MJ. Regionally specific loss of neurons in the aging human hippocampus. Neurobiol Aging. 1993; 14:287–293. [PubMed: 8367010]

Williams C, Mehrian Shai R, Wu Y, Hsu YH, Sitzer T, Spann B, McCleary C, Mo Y, Miller CA. Transcriptome analysis of synaptoneurosomes identifies neuroplasticity genes overexpressed in incipient Alzheimer's disease. PLoS One. 2009; 4:e4936. [PubMed: 19295912]

Highlights

- Hippocampal CA1 neurons display widespread synaptic gene downregulation in MCI and AD
- Genes encoding APP and APP family members were unaffected in MCI and AD
- Synaptic mRNA levels correlate with poorer cognition and increased AD pathology
- CA1 synaptic dysregulation is a very early pathogenic event in AD

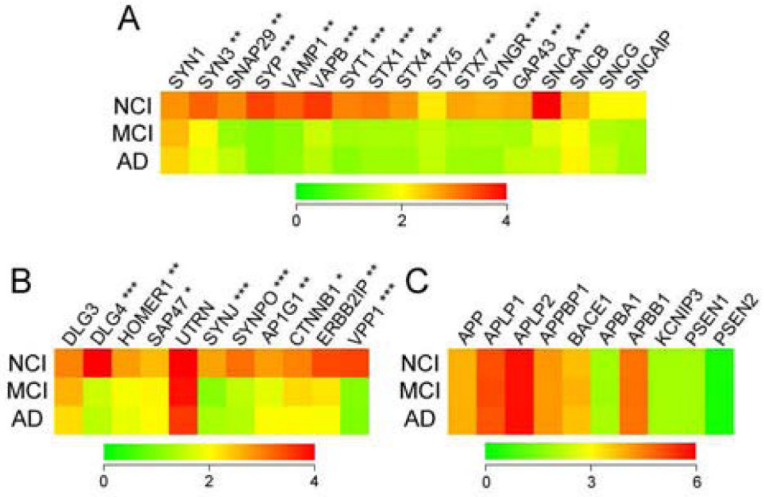

Figure 1.

Color-coded heatmaps demonstrate the dysregulation of synaptic transcripts compared to APP-related transcripts in CA1 neurons in MCI and mild/moderate AD. A) Quantitative analysis of relative gene expression levels revealed that 12 of the 17 synaptic transcripts on the custom microarrays which regulate presynaptic function were significantly down-regulated (red-to-green) in CA1 neurons in MCI compared to NCI. Note that levels of these transcripts were equivalent in CA1 neurons from MCI and AD cases. B) Likewise, nine of 11 transcripts regulating either postsynaptic function or clathrin-mediated synaptic endocytosis were significantly down-regulated in MCI and AD relative to NCI. C) By contrast, transcripts for APP, APP-like proteins, and APP binding proteins or processing enzymes were stable across the clinical diagnostic groups. *$p < 01$, **$p < 0.001$, ***$p < 0.0001$ via one-way ANOVA with Newman-Keuls *post hoc* test for multiple comparisons. Abbreviations: SYN1, synapsin 1; SYN3, synapsin 3, SNAP29, synaptosomal-associated protein, 29 kDa; SYP, synaptophysin; VAMP1, vesicle-associated membrane protein 1, or synaptobrevin 1; VPB, VAMP-associated protein B; SYT1, synaptotagmin 1; STX1, 4, 5, 7, syntaxin 1, 4, 5, 7; SYNGR, synaptogyrin; GAP43, growth-associated protein, 43 kDa; SNCA, α-synuclein; SNCB, β-synuclein; SNCG, γ-synuclein; SNCAIP, α-synuclein-interacting protein; DLG3, Discs, Large Homolog 3 or synapse-associated protein, 102 kDa (SAP102); DLG4, Discs, Large Homolog 4 or postsynaptic density protein, 95 kDa (PSD95), HOMER1, Homer homolog 1; SAP47, synapse-associated protein, 47 kDa; UTRN, utrophin; SYNJ, synaptojanin; SYNPO, synaptopodin; AP1G1, adaptor-related protein complex 1, γ1 subunit; CTNNB1, β-catenin; ERBB2IP, Erb-B2, or Human Epidermal Growth Factor Receptor 2-interacting protein; VPP1, vesicle proton pump, 116 kDa; APP, β-amyloid precursor protein; APLP1, APP-like protein 1; APLP2, APP-like protein 2; APPBP1, APP-binding protein 1 or NEDD8 Activating Enzyme; BACE 1, beta-site APP-cleaving enzyme 1; APBA1, APP-binding A1 protein; APBB1, APP-binding B1 protein; KCNIP3, Kv protein-interacting channel 3, or calsenilin; PSEN1, 2, presenilin 1, 2.

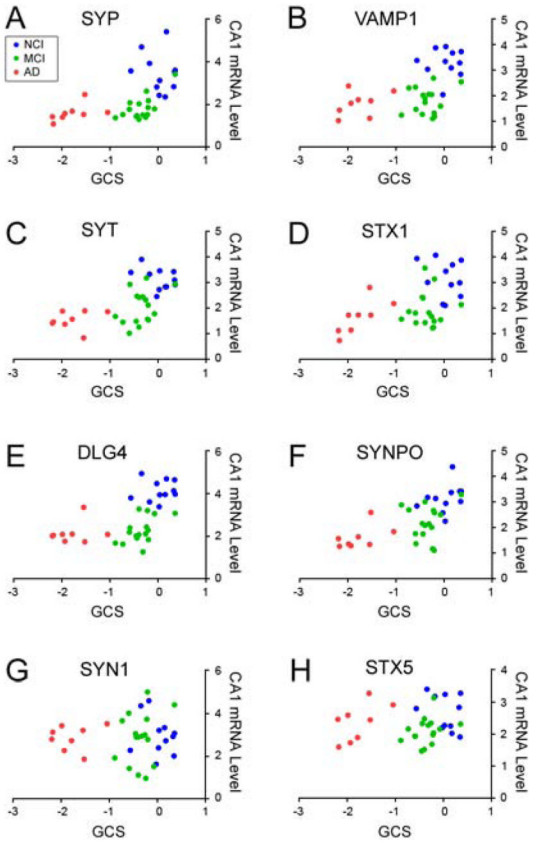

Figure 2.

Scattergrams show that downregulation of select synaptic transcripts in CA1 neurons correlates with poorer global cognitive performance. Relative expression levels for specific CA1 synaptic transcripts were plotted against the global cognitive score (GCS, or *z*-score of 19 neuropsychological tests, see Methods) for each Religious Orders Study subject under analysis. For each panel, individual cases are color-coded for NCI (blue), MCI (green), or mild/moderate AD (red). Note that for the GCS scale, the more negative the *z*-score, the poorer the performance on the battery of cognitive tests. Spearman rank correlations for the select transcripts are as follows: A) synaptophysin (SYP), $r = 0.66$, $p < 0.0001$; B) synaptobrevin (VAMP1), $r = 0.55$, $p = 0.0006$; C) synaptotagmin (SYT), $r = 0.64$, $p < 0.0001$; D) syntaxin 1 (STX1), $r = 0.49$, $p = 0.003$; E) Discs, Large Homolog 4 (DLG4, or PSD95), $r = 0.66$, $p < 0.0001$; F) synaptopodin (SYNPO), $r = 0.67$, $p < 0.0001$; synapsin 1 (SYP1), $r = 0.04$, $p = 0.8$; syntaxin 5 (STX5), $r = 0.18$, $p = 0.3$.

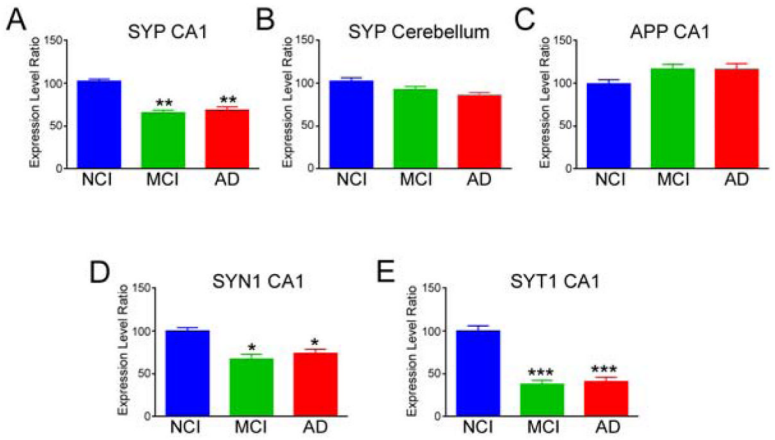

Figure 3.

qPCR validation of CA1 neuronal synaptophysin (SYP) and APP (APP) expression profiling. A, B) Quantitative analysis of SYP mRNA normalized to GAPDH mRNA levels as determined by qPCR analysis of frozen hippocampal CA1 (A) and cerebellar (B) tissue. C) Quantitative analysis of APP mRNA normalized to GAPDH mRNA levels as determined by qPCR analysis of frozen hippocampal CA1 tissue. D, E) Quantitative analysis of SYN1 (D) and SYT1 (E) mRNA normalized to GAPDH mRNA levels as determined by qPCR analysis of frozen hippocampal CA1 tissue. *, $p < 0.05$, **, $p < 0.01$, ***, $p < 0.001$ via Kruskall-Wallis with *post hoc* Bonferroni test for multiple comparisons.

Neuropharmacology. Author manuscript; available in PMC 2015 April 01.

Table 1

Clinical, demographic, and neuropathological characteristics by diagnosis category

		Clinical Diagnosis			P-value	Pair-wise comparisons*
		NCI (N=12)	MCI (N=15)	AD* (N=8)		
Age (years) at death:	Mean ± SD (Range)	84.4 ± 6.0 (72-92)	86.2 ± 5.2 (80-97)	88.2 ± 7.0 (80-101)	0.4[a]	--
Number (%) of males:		6 (50%)	6 (40%)	3 (37.5%)	0.9[b]	--
Years of education:	Mean ± SD (Range)	16.9 ± 4.0 (15-21)	18.9 ± 2.3 (16-22)	17.1 ± 1.5 (16-20)	0.1[a]	--
Number (%) with ApoE ε4 allele:		2 (18%)	6 (40%)	6 (75%)	0.02[b]	(NCI, MCI) < AD
MMSE:	Mean ± SD (Range)	27.8 ± 1.5 (25-30)	26.7 ± 2.7 (20-30)	19.1 ± 1.3 (15-25)	<0.0001[a]	(NCI, MCI) > AD
GCS:	Mean ± SD (Range)	0.04 ± 0.3 (−0.6-0.4)	−0.4 ± 0.2 (−0.9- -0.07)	−1.8 ± 0.4 (−2.2- -1.1)	<0.0001[a]	NCI > MCI > AD
Post-mortem interval (hours):	Mean ± SD (Range)	5.4 ± 2.7 (2.3-11)	6.7 ± 4.2 (3-16)	7.1 ± 4.0 (2.2-12)	0.5[a]	--
Distribution of Braak scores:	0	0	0	0		
	I/II	6	1	1	0.004[c]	NCI < (MCI, AD)
	III/IV	6	10	1		
	V/VI	0	4	6		
NIA Reagan diagnosis	No AD	0	0	0		
(likelihood of AD):	Low	9	3	1	0.002[c]	NCI < (MCI, AD)
	Intermediate	3	10	2		
	High	0	2	5		
CERAD diagnosis:	No AD	6	1	0		
	Possible	2	2	0	0.006 [c]	NCI < (MCI, AD)
	Probable	3	5	4		
	Definite	1	7	4		

[a] one-way ANOVA

[b] Fisher's exact test

[c] Kruskal-Wallis test

* Bonferroni correction

Table 2

Clinical pathologic correlations of select CA1 synaptic transcripts

synaptic gene	MMSE	Braak	NIA-Reagan	CERAD
syp	$r = 0.37$ ($p = 0.03$)	$r = -0.50$ ($p = 0.003$)	$r = -0.41$ ($p = 0.02$)	$r = -0.40$ ($p = 0.01$)
vamp1	$r = 0.36$ ($p = 0.03$)	$r = -0.51$ ($p = 0.002$)	$r = -0.35$ ($p = 0.04$)	$r = -0.50$ ($p = 0.003$)
syt1	$r = 0.46$ ($p = 0.005$)	$r = -0.42$ ($p = 0.01$)	$r = -0.42$ ($p = 0.01$)	$r = -0.39$ ($p = 0.02$)
stx1	$r = 0.33$ ($p = 0.06$)	$r = -0.43$ ($p = 0.01$)	$r = -0.20$ ($p = 0.2$)	$r = -0.32$ ($p = 0.05$)
dlg4	$r = 0.35$ ($p = 0.04$)	$r = -0.55$ ($p < 0.001$)	$r = -0.50$ ($p = 0.005$)	$r = -0.55$ ($p = 0.006$)
synpo	$r = 0.54$ ($p = 0.0007$)	$r = -0.63$ ($p < 0.001$)	$r = -0.56$ ($p = 0.005$)	$r = -0.55$ ($p = 0.006$)
homer1	$r = 0.34$ ($p = 0.04$)	$r = -0.62$ ($p < 0.001$)	$r = -0.58$ ($p = 0.003$)	$r = -0.41$ ($p = 0.01$)
syn1	$r = 0.11$ ($p = 0.5$)	$r = -0.18$ ($p = 0.6$)	$r = -0.09$ ($p = 0.6$)	$r = -0.28$ ($p = 0.1$)
stx5	$r = 0.02$ ($p = 0.9$)	$r = -0.05$ ($p = 0.8$)	$r = -0.04$ ($p = 0.8$)	$r = -0.12$ ($p = 0.5$)